

Optimizing potential energy functions for maximal intrinsic hyperpolarizability

Juefei Zhou,¹ Urszula B. Szafruga,¹ David S. Watkins,^{1,2} and Mark G. Kuzyk¹

¹*Department of Physics and Astronomy, Washington State University, Pullman, Washington 99164-2814, USA*

²*Department of Mathematics, Washington State University, Pullman, Washington 99164-3113, USA*

(Received 18 April 2007; published 28 November 2007)

We use numerical optimization to study the properties of (1) the class of one-dimensional potential energy functions and (2) systems of point nuclei in two dimensions that yield the largest intrinsic hyperpolarizabilities, which we find to be within 30% of the fundamental limit. In all cases, we use a one-electron model. It is found that a broad range of optimized potentials, each of very different character, yield the same intrinsic hyperpolarizability ceiling of 0.709. Furthermore, all optimized potential energy functions share common features such as (1) the value of the normalized transition dipole moment to the dominant state, which forces the hyperpolarizability to be dominated by only two excited states and (2) the energy ratio between the two dominant states. All optimized potentials are found to obey the three-level ansatz to within about 1%. Many of these potential energy functions may be implementable in multiple quantum well structures. The subset of potentials with undulations reaffirm that modulation of conjugation may be an approach for making better organic molecules, though there appear to be many others. Additionally, our results suggest that one-dimensional molecules may have larger diagonal intrinsic hyperpolarizability β_{xxx}^{int} than higher-dimensional systems.

DOI: 10.1103/PhysRevA.76.053831

PACS number(s): 42.65.An, 11.55.Hx, 33.15.Kr, 33.55.-b

I. INTRODUCTION

Materials with large nonlinear-optical susceptibilities are central for optical applications such as telecommunications [1], three-dimensional nanophotolithography [2,3], and making materials [4] for cancer therapies [5]. The fact that quantum calculations show that there is a limit to the nonlinear-optical response [6–11] is both interesting from the basic science perspective and provides a target for making optimized materials. In this work, we focus on the second-order susceptibility and the underlying molecular hyperpolarizability, which is the basis of electro-optic switches and frequency doublers.

The fundamental limit of the off-resonance hyperpolarizability is given by [8]

$$\beta_{\text{max}} = \sqrt[4]{3} \left(\frac{e\hbar}{\sqrt{m}} \right)^3 \frac{N^{3/2}}{E_{10}^{7/2}}, \quad (1)$$

where N is the number of electrons and E_{10} the energy difference between the first excited state and the ground state $E_{10}=E_1-E_0$. Using Eq. (1), we can define the off-resonant intrinsic hyperpolarizability β_{int} as the ratio of the actual hyperpolarizability (measured or calculated) β to the fundamental limit

$$\beta_{\text{int}} = \beta/\beta_{\text{max}}. \quad (2)$$

We note that since the dispersion of the fundamental limit of β is also known [12] it is possible to calculate the intrinsic hyperpolarizability at any set of wavelengths for any second-order phenomena. In the present work, we treat only the zero-frequency limit.

Until recently, the largest nonlinear susceptibilities of the best molecules fell short of the fundamental limit by a factor of $10^{3/2}$ [10,13,14] so the very best molecules had a value of $\beta_{\text{int}}=0.03$. Since a sum-over-states (SOS) calculation of the hyperpolarizability [15] using the analytical wave functions of the clipped harmonic oscillator yields a value $\beta_{\text{int}}=0.57$

[14], the factor-of-30 gap is not of a fundamental nature. Indeed, recently, it was reported that a molecule with asymmetric conjugation modulation has a measured value of $\beta_{\text{int}}=0.048$ [16].

To investigate how one might make molecules with a larger intrinsic hyperpolarizability, Zhou and co-workers used a numerical optimization process where a trial potential energy function is entered as an input, and the code iteratively deforms the potential energy function until the intrinsic hyperpolarizability, calculated from the resulting wave functions, converges to a local maximum [17]. In this work, a hyperbolic tangent function was used as the starting potential due to the fact that it is both asymmetric yet relatively flat away from the origin. This calculation was one-dimensional and included only one electron, so electron correlation effects were ignored. Furthermore, the intrinsic hyperpolarizability was calculated using the dipole-free sum-over-states expression [18] and only 15 excited states were included. The resulting optimized potential energy function showed strong oscillations, which served to separate the spatial overlap between the energy eigenfunctions. This led Zhou and co-workers to propose that modulated conjugation in the bridge between donor and acceptor ends of such molecules may be a paradigm for making molecules with higher intrinsic hyperpolarizability [17].

Based on this paradigm, Pérez Moreno reported measurements of a class of chromophores with varying degree of modulated conjugation [16]. The best measured intrinsic hyperpolarizability was $\beta_{\text{int}}=0.048$, about 50% larger than the best previously reported. Given the modest degree of conjugation modulation for this molecule, this paradigm shows promise for further improvements.

In the present work, we extend Zhou's calculations to a larger set of starting potentials. To circumvent truncation problems associated with sum-over-states calculations, we instead determine the hyperpolarizability using a finite difference technique. The optimization procedure is then applied to this nonperturbative hyperpolarizability.

To study the effects of geometry on the hyperpolarizability, Kuzyk and Watkins calculated the hyperpolarizability of various arrangements of point charges, representing nuclei, in two dimensions using a two-dimensional Coulomb potential [19]. In the present contribution, we apply our numerical optimization technique to determine the arrangement and charges of the nuclei in a planar molecule that maximizes the intrinsic hyperpolarizability.

II. THEORY

In our previous work, we used a finite-state SOS model of the hyperpolarizability that derives from perturbation theory (we used both the standard Orr and Ward SOS expression β_{SOS} [15] and the other dipole free expression β_{DF} [18]). The use of a finite number of states in lieu of the full infinite sums can result in inaccuracies so, in the present work, we use the nonperturbative approach, as follows. We begin by solving the one-dimensional (1D) Schrödinger equation on the interval $a < x < b$ for the ground-state wave function $\psi(x, E)$ of an electron in a potential well defined by $V(x)$ and in the presence of a static electric field E that adds to the potential $\delta V = -exE$. From this, the off-resonant hyperpolarizability is calculated with numerical differentiation, i.e., using finite differences, yielding

$$\beta_{\text{NP}} = \frac{1}{2} \left. \frac{\partial^2 \left[- \int_a^b |\psi(x, E)|^2 ex dx \right]}{\partial E^2} \right|_{E=0}. \quad (3)$$

Equation (3) is evaluated using the standard second-order approximation to the second derivative

$$f''(z) \approx \frac{f(z+h) - 2f(z) + f(z-h)}{h^2}$$

with several h values $h_0, h_0/5, h_0/25, \dots$. We then refine these values by Richardson extrapolation [20] and obtain our estimate from the two closest extrapolated values. The error of our estimates is of order h^4 , so we can estimate second derivatives as accurately as we please in principle by taking h sufficiently small. In practice we are limited by roundoff errors, which become larger as h is decreased. Our estimates are correct to about seven decimal places.

Our computational mesh consists of 200 quadratic finite elements with a total of 399 degrees of freedom. The potential energy function is a cubic spline with 40 degrees of freedom. Thus the numerical calculations in regions where the potential function is represented by 3 points in the spline are covered by 15 elements with a total of about 30 degrees of freedom. Consequently the finite element mesh is sufficiently fine to capture all details of the potential function accurately. As a test we repeated several runs with a refined mesh with 400 finite elements and 799 degrees of freedom. All results for the refined mesh agreed with those for the original mesh to at least six decimal places.

Calculating β_{int} from Eqs. (3), (2), and (1) for a specific potential, we use an optimization algorithm that continuously varies the potential in a way that maximizes β_{int} . We also compute the matrix [17,21]

$$\tau_{mp}^{(N)} = \delta_{m,p} - \frac{1}{2} \sum_{n=0}^N \left(\frac{E_{nm}}{E_{10}} + \frac{E_{np}}{E_{10}} \right) \frac{x_{mn}^{\text{max}} x_{np}^{\text{max}}}{x_{10}^{\text{max}} x_{10}^{\text{max}}}, \quad (4)$$

where x_{10}^{max} is the magnitude of the fundamental limit of the position matrix element x_{10} for a one-electron system and is given by

$$x_{10}^{\text{max}} = \frac{\hbar}{\sqrt{2mE_{10}}}. \quad (5)$$

Each matrix element of $\tau^{(N)}$, indexed by m and p , is a measure of how well the (m, p) sum rule is obeyed when truncated to N states. If the sum rules are exactly obeyed, $\tau_{mp}^{(\infty)} = 0$ for all m and p . We note that if the sum rules are truncated to an N -state model, the sum rules indexed by a large value of m or p (i.e., $m, p \sim N$) may be disobeyed even when the position matrix elements and energies are exact. We have found that the values of $\tau_{mp}^{(N)}$ are small for exact wave functions when $m < N/2$ and $p < N/2$. So, when evaluating the τ matrix to test our calculations, we consider only the components $\tau_{m \leq N/2, p \leq N/2}^{(N)}$.

We observe that when using more than about 40 states in SOS calculations of the hyperpolarizability only a marginal increase of accuracy results when the potential energy function is parametrized with 400 degrees of freedom. So, to ensure overkill, we use 80 states when calculating the τ matrix or the hyperpolarizability with an SOS expression so that truncation errors are kept to a minimum. Since the hyperpolarizability depends critically on the transition dipole moment from the ground state to the excited states, we use the value of $\tau_{00}^{(40)}$ as one important test of the accuracy of the calculated wave functions. Additionally, we use the standard deviation of $\tau^{(N)}$,

$$\Delta \tau^{(N)} = \frac{\sqrt{\sum_{m=0}^{N/2} \sum_{p=0}^{N/2} (\tau_{mp}^{(N)})^2}}{N/2}, \quad (6)$$

which quantifies, on average, how well the sum rules are obeyed in aggregate, making $\Delta \tau^{(N)}$ a broader test of the accuracy of a large set of wave functions.

Our code is written in MATLAB. For each trial potential we use a quadratic finite element method [22] to approximate the Schrödinger eigenvalue problem and the implicitly restarted Arnoldi method [23] to compute the wave functions and energy levels. To optimize β we use the Nelder-Mead simplex algorithm [24].

As described in our previous work [17], we perform optimization, but this time using the exact intrinsic hyperpolarizability $\beta = \beta_{\text{NP}} / \beta_{\text{max}}$, where β_{max} is the fundamental limit of the hyperpolarizability, which is proportional to $E_{10}^{7/2}$. To determine $E_{10} \equiv E_1 - E_0$, we also calculate the first excited state energy E_1 .

III. RESULTS AND DISCUSSIONS

Figure 1 shows an example of the optimized potential energy function after 7000 iterations when starting with the

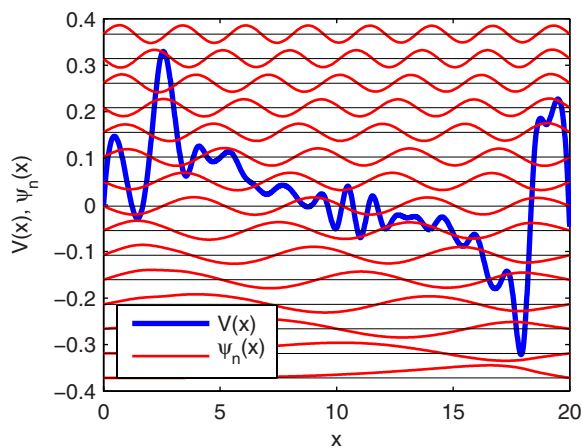


FIG. 1. (Color online) Optimized potential energy function and first 15 wave functions after 7000 iterations. The starting potential is $V(x)=0$ using the nonperturbative hyperpolarizability for optimization.

potential $V(x)=0$ and optimizing the nonperturbative intrinsic hyperpolarizability $\beta_{\text{NP}}/\beta_{\text{max}}$ as calculated with Eq. (3). Also shown are the eigenfunctions of the first 15 states computed from the optimized potential. First, we note that the potential energy function shows the same kinds of wiggles as in our original paper [17], though not of sufficient amplitude to localize the wave functions.

For the starting potentials we have investigated, our results fall into two broad classes. In the first, three common features are (1) the best intrinsic hyperpolarizabilities are near $\beta_{\text{int}}=0.71$, (2) the best potentials have a series of wiggles, and (3) the systems behave as a limited-state model. In the second class of starting potentials, (1) the optimized intrinsic hyperpolarizability is near $\beta_{\text{int}}=0.71$, (2) the wiggles are much less pronounced, and (3) many eigenfunctions overlap but only three states contribute to the hyperpolarizability. Figure 1 is an example of a class II potential. However, in both classes, the maximum calculated intrinsic hyperpolarizability appears to be bounded by $\beta_{\text{int}}=0.71$. Using the set of potentials from both classes that lead to optimized $\beta_{\text{NP}}/\beta_{\text{max}}$, we calculate the lowest 80 eigenfunctions and eigenvalues, from which we calculate β_{DF} and β_{SOS} . In most cases, we find that the three different formulas for β converge to the same value when only the first 20 excited states are used (using 80 states, the three are often the same to within at least 4 decimal places) and $\tau_{00} \approx 10^{-4}$, showing that the ground state sum rules are well obeyed. Furthermore, the root-mean-square (rms) deviation of the τ matrix when including 40 states leads to $\tau^{(80)} < 0.001$.

Figure 2 shows an example of the optimized potential energy function when starting with the potential $V(x)=\tanh(x)$ and optimizing the exact (nonperturbative) intrinsic hyperpolarizability. Also shown are the eigenfunctions of the first 15 states computed with the optimized potential. First, we note that the potential energy function shows the same kinds of wiggles as in our original paper [17] and only two excited state wave functions and the ground state are localized in the first deep well—placing this system in class I.

The observation that such potentials lead to hyperpolarizabilities that are near the fundamental limit motivated Zhou

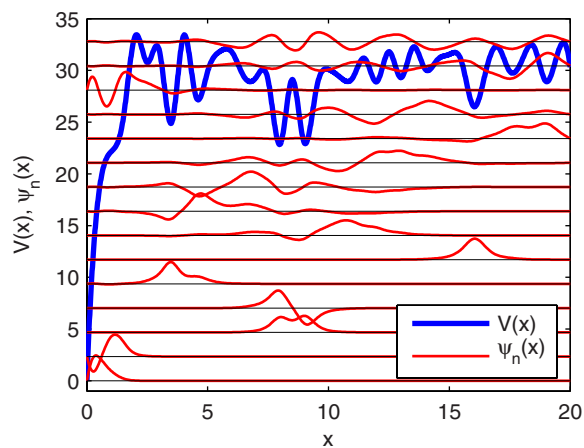


FIG. 2. (Color online) Optimized potential energy function and first 15 wave functions after 8000 iterations. The starting potential is $V(x)=\tanh(x)$, using the nonperturbative hyperpolarizability for optimization.

and co-workers to suggest that molecules with modulated conjugation may have enhanced intrinsic hyperpolarizabilities [17]. A molecule with a modulated conjugation bridge between the donor and acceptor end was later shown to have record-high intrinsic hyperpolarizability [16]. As such, this result warrants a more careful analysis.

It is worthwhile to compare our present results characterized by Fig. 2 with our past work [17], particularly for the purpose of examining the impact of the approximations used in the previous work [17]. Figure 3 shows the optimized potential and wave functions obtained by Zhou and co-workers using a 15-state model and optimizing the dipole-free intrinsic hyperpolarizability. Since only 15 states were used, the SOS expression for β did not fully converge; making the result inaccurate as suggested by the fact that β_{SOS} and β_{DF} did not agree (for the rest of the document, all stated hyperpolarizabilities are intrinsic hyperpolarizabilities unless explicitly stated to the contrary). However, since the code focused on optimizing the dipole-free form of β , and τ_{00} was

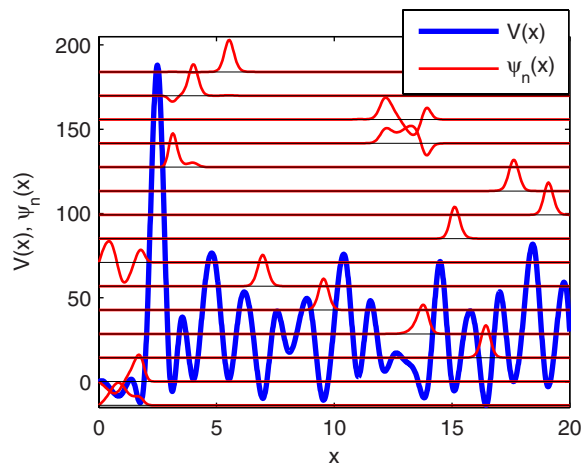


FIG. 3. (Color online) Optimized potential energy function using β_{DF} and the first 15 wave functions after 7000 iterations. The starting potential is the $\tanh(x)$ potential. The final potential (shown above) we refer to as the partially optimized tanh potential (POTP).

TABLE I. Evolution of the POTP potential. β_S is the hyperpolarizability of the starting potential using 80 states while the other ones are after optimization of β_{NP} .

Number of Iterations	β_S	β_{SOS}	β_{DF}	β_{NP}	$\tau_{00}^{(80)}$ ($\times 10^{-5}$)	$\Delta\tau^{(80)}$ ($\times 10^{-4}$)
0	0.5612	0.5612	0.5607	0.5612	11.2	15
1000	0.5612	0.7087	0.6682	0.7083	1810	40

small when β_{int} was optimized, the dipole-free expression may have converged to a reasonably accurate value while the commonly used SOS expression was inaccurate. Indeed, it was found that $\beta_{DF} \approx 0.72$ —in contrast to our more precise present calculations using the nonperturbative approach, which yields $\beta_{NP} < 0.71$. So, the fact that our more precise calculations, which do not rely on a sum-over states expression, agree so well with the 15-state model suggests that in both cases, the limit for a one-dimensional single electron molecule is just over $\beta \approx 0.7$. This brute force calculation serves as a numerical illustration of the observation that the upper bound of β is the same for an exact nonperturbation calculation and for a calculation that truncates the SOS expression, which presumably should lead to large inaccuracies [25,26]. At minimum, this result supports the existence of fundamental limits of nonlinear susceptibilities that are in line with past calculations.

To state Zhou's approach more precisely [17], the calculations optimized the very special case of the intrinsic hyperpolarizability for a 15 state model for a potential energy function that is parametrized with 20 spline points. As such, the potential energy function can at most develop about 20 wiggles. As a consequence, there are enough degrees of freedom in the potential energy function to force the 15 states to be spatially well separated. Interestingly, after optimization, only two excited states overlap with the ground state, allowing only these two states to have nonzero transition dipole moments with each other and the ground state—forcing the system into a three-level SOS model for β_{DF} . This behavior is interesting in light of the three-level ansatz, which asserts that only three states determine the nonlinear response of a system when it is near the fundamental limits.

It is interesting to compare the exact nonperturbation calculation, which does not depend on the excited state wave functions (Fig. 2) and Zhou's contrived system of 15 states (Fig. 3). Both cases have wiggles and the wave functions appear to be mostly nonoverlapping. So, for the first 15 states, the wave functions appear similarly localized. The situation becomes more interesting when 80 states are included in calculating the hyperpolarizability for the partially optimized tanh potential (POTP) or when the exact nonperturbative approach is used. The first line in Table I summarizes the results with the POTP potential and 80 states.

First, let us focus on the sum-over-states results. Clearly, when 80 states are used in the calculation, it is impossible for the excited state wave functions to not overlap with each other, so the three-level approximation to β breaks down. According to the three-level ansatz, we would expect the hyperpolarizability to get smaller. Indeed, the additional excited states result in a smaller hyperpolarizability (≈ 0.56).

Note that the exact and SOS expressions agree with each other and that $\tau_{00}^{(80)}$ and $\Delta\tau^{(80)}$ are small.

Figure 4 shows the result after 1000 iterations, using the POTP potential as the starting potential and using the nonperturbative hyperpolarizability for optimization. First, the nonperturbative hyperpolarizability reaches just under 0.71, but, the SOS and dipole-free expressions do not agree with each other. Furthermore, both convergence metrics ($\tau_{00}^{(80)}$ and $\Delta\tau^{(80)}$) are larger than before optimization. It would appear that for the POTP potential, even 80 states are not sufficient to characterize the nonlinear susceptibility when a sum-over-states expression is used (either dipole free or traditional SOS expression—though the SOS expression agrees better with the nonperturbative approach). This is the only case that we have observed where the three expressions for the hyperpolarizability disagree when 80 states are used.

Interestingly, the optimized potential energy function still retains the wiggles and the wave functions are still well separated. This result is consistent with the suggestion of Zhou and co-workers that modulation of conjugation may be a good design strategy for making large-hyperpolarizability molecules. We note that wiggles in the potential energy function are not required to get a large nonlinear-optical response but appears to be one way that Mother Nature optimizes the hyperpolarizability. Since this idea has been used to identify molecules with experimentally measured record intrinsic hyperpolarizability [16] the concept of modulation of conjugation warrants further experimental studies.

As a case in point that non-wiggly potentials can lead to a large nonlinear susceptibility is the clipped harmonic oscil-

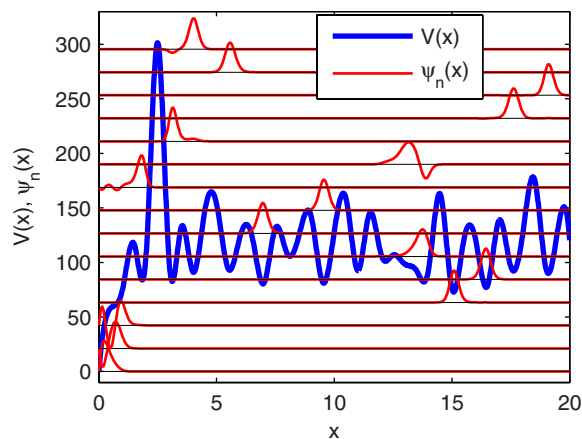


FIG. 4. (Color online) Optimized potential energy function and first 15 wave functions after 1000 iterations. The starting potential is the POTP potential, using the nonperturbative hyperpolarizability for optimization.

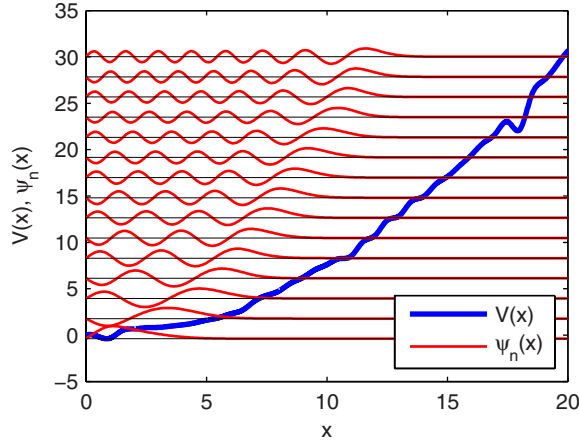


FIG. 5. (Color online) Optimized potential energy function and first 15 wave functions after 8000 iterations. The starting potential is $V(x)=x^2$, using the nonperturbative hyperpolarizability for optimization.

lator, which we calculated to have an intrinsic hyperpolarizability of about 0.57 [14]. Figure 5 shows the optimized nonperturbative hyperpolarizability when using a clipped harmonic oscillator as the starting potential. The properties of all of the optimized potentials are summarized in Table II. The clipped square root function also has a large hyperpolarizability (0.69). The optimized potential is shown in Fig. 6. In these cases, the amplitude of the wiggles are small and all the wave functions overlap. So, these fall into class II. Note that the lack of wiggles shows that wiggles are not an inevitable consequence of our numerical calculations.

We may question whether small wiggles in the potential energy function lead to large amplitude wiggles as an artifact of our numerical optimization technique. To test this hypothesis, we used the trial potential energy function $x+\sin(x)$, where the wiggle amplitude is not large enough to cause the wave functions to localize at the minima. The optimized potential energy function retains an approximately linear form with only small fluctuation. In fact, the results are very similar to what we found for the linear starting potential and the wiggles do not affect the final result. The similarity between these cases can be seen in Table II.

TABLE II. Summary of calculations with different starting potentials. β_s is the hyperpolarizability of the starting potential while the other ones are after optimization. The transition moments and energies are in dimensionless units. To convert to specific units, consider an example where x_{nm} is interpreted to be in units of Å. The energies would then be determined by multiplying all values of E_{n0} by \hbar^2/ma^2 , with $a=10^{-10}$ m (1 Å). In this case, the energy is in units of 1.2×10^{-18} J or about 7.6 eV.

Function $V(x)$	β_S	β_{SOS}	β_{DF}	β_{NP}	$\tau_{00}^{(80)}$ ($\times 10^{-4}$)	$\Delta\tau^{(80)}$ ($\times 10^{-4}$)	E_{10}	E_{20}	x_{00}	x_{10}	x_{20}	x_{11}	x_{21}	x_{22}	$\frac{x_{01}}{x_{max}}$
0	0	0.7089	0.7089	0.7089	3.78	5.33	0.0817	0.168	15.362	1.951	0.658	10.923	2.840	9.283	0.789
$30 \tanh(x)$	0.67	0.7084	0.6918	0.7083	77.9	11.8	5.474	11.217	0.510	0.2387	0.077	1.051	0.332	1.447	0.790
x	0.66	0.7088	0.7072	0.7088	7.87	8.79	1.4575	2.983	0.997	0.462	0.155	2.049	0.671	2.477	0.789
x^2	0.57	0.7089	0.7085	0.7088	1.86	703	0.6643	1.364	1.522	0.684	0.321	3.079	0.996	3.646	0.789
$x^{1/2}$	0.68	0.7087	0.7049	0.7087	19.0	9.76	2.2948	4.677	0.783	0.368	0.122	1.621	0.533	2.011	0.789
$x+\sin(x)$	0.67	0.7088	0.7073	0.7088	7.50	8.46	1.3080	2.673	1.044	0.488	0.163	2.154	0.708	2.625	0.789
$x+10 \sin(x)$	0.04	0.7085	0.7085	0.7085	0.165	7.78	1.734	3.576	4.463	0.424	0.143	3.501	0.613	3.126	0.790

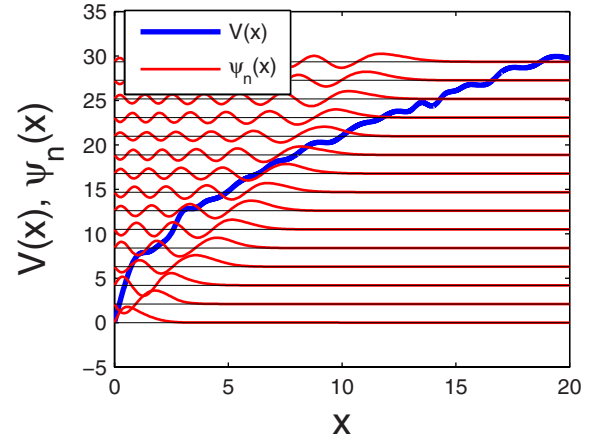


FIG. 6. (Color online) Optimized potential energy function and first 15 wave functions after 8000 iterations. The starting potential is $V(x)=\sqrt{x}$, using the nonperturbative hyperpolarizability for optimization.

Next, we test a starting potential with large wiggles as shown in the upper portion of Fig. 7. The lower-energy eigenfunctions are found to be localized mostly in the first two wells. In fact, the lowest four energy eigenfunctions are well approximated by harmonic oscillator wave functions, which are approximately eigenstates of parity due to the locally centrosymmetric potential. As a result, the first excited state holds most of the oscillator strength and the value of the intrinsic hyperpolarizability is only 0.04.

After 3000 interactions, this class I potential energy function has high amplitude wiggles at a wavelength that is significantly shorter than the wavelength of the initial sine function (bottom portion of Fig. 7). In common with the optimized $\tanh(x)$ function, the wiggles are of large but almost chaotically varying amplitude. This leads to wave functions that are spatially separated. While the wave functions are not as well separated as we find for the $\tanh(x)$ starting potential, the optimized potential yields only two dominant transition from the ground state; so, this system is well approximated by a three-level model. As is apparent from Table II, the ground state sum rule (characterized by $\tau_{00}^{(80)}$) is better obeyed in this optimized potential than in any others. So, the

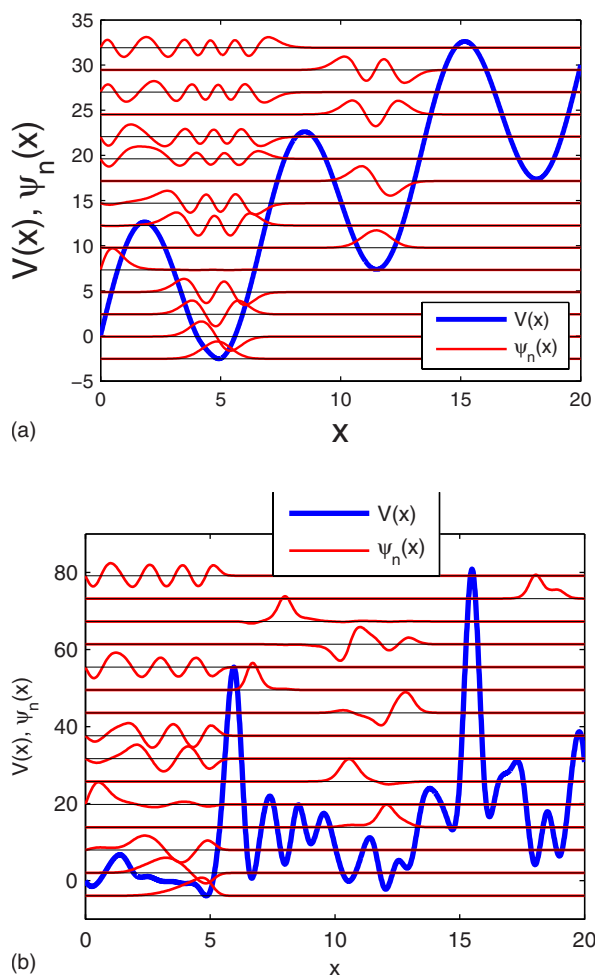


FIG. 7. (Color online) Potential energy function and first 15 wave functions before (top) and after (bottom) 3000 iterations. The starting potential is of the form $V(x)=x+10 \sin(x)$, using the non-perturbative hyperpolarizability for optimization.

wave functions are accurate and all of the values of β have converged to the same value, suggesting that this calculation may be the most accurate of the set.

Our results bring up several interesting questions. First, all of our extensive numerical calculations, independent of the starting potential, yield an optimized intrinsic hyperpolarizability with an upper bound of 0.71, which is about 30% lower than what the sum rules allow. Since numerical optimization can settle in to a local maximum, it is possible that all of the starting potentials are far from the global maximum of $\beta_{\text{int}}=1$. Indeed, since most starting potentials lead to systems that require more than three dominant states to express the hyperpolarizability, this may in itself be an indicator that we are not at the fundamental limit precisely because these systems have more than three states. Indeed, the original results of Zhou and co-workers frames the problem in a way (i.e., a 15-level model in a potential limited to about 20 wiggles) that allows a solution to the optimization problem to lead to three dominant states. So, while it may be argued that this system is contrived and unphysical, we have found value in trying such toy models when testing various hypo-

theses. This toy model leads to a three-level system as the three-level ansatz proposes, has the same qualitative properties as more precise methods, and has given insights into making molecules with record-breaking intrinsic hyperpolarizability. Given the complexity of calculating nonlinear-susceptibilities, our semiquantitative method may be a good way of generating ideas.

The three-level ansatz proposes that at the fundamental limit, all transitions are negligible except between three dominant states. There appears to be no proof of the ansatz aside from the fact that it leads to an accurate prediction of the upper bound of nonlinear susceptibilities, both calculated and measured. To understand the motivation behind the ansatz, it is useful to understand how the two-level model optimizes the polarizability α without the need to rely on any assumptions. This is trivial to show by using the fact that the polarizability depends only on the positive-definite square of transition moments $\langle 0|x|n\rangle\langle n|x|0\rangle$, the same parameters that are found in the ground-state sum rules [21].

For nonlinear susceptibilities, the situation is much more complicated because the SOS expression depends on quantities such as $\langle 0|x|n\rangle\langle n|x|m\rangle\langle m|x|0\rangle$, where these terms can be both positive and negative. Furthermore, the sum rules that relate excited states moments to each other allow for these moments to be much larger than transition moments to the ground state. So, it would seem plausible that one could design a system with many excited states in a way that all of the transition moments between excited states would add constructively to yield a larger hyperpolarizability than what we calculate with the three-level ansatz. None of our numerical calculations, independent of the potential energy function, yield a value greater than 0.71. Since our potential energy functions are general one-dimensional potentials (i.e., the potentials are not limited to Coulomb potentials nor are the wave functions approximated as is common in standard quantum chemical computations), our calculations most likely span a broader range of possible wave functions leading to a larger variety of states that contribute to the hyperpolarizability.

However, there appear to be local maxima associated with systems that behave as a three-level system and others with many states, and, the maximum values both are 0.71. It is interesting that so many different sets of transition moments and energies can yield the exact same local maximum. To gain a deeper appreciation of the underlying physics, let us consider the transition moments and energies in the sum-over-states expression for the hyperpolarizability as adjustable parameters. For a system with N states, there are $N-1$ energy parameters of the form E_n-E_0 . The moment matrix x_{ij} has N^2 components. If the matrix is real, there are $(N^2-N)/2$ unique off-diagonal terms and N diagonal dipole moments. Since all dipole moments appear as differences of the form $x_{nm}-x_{00}$, there are only $N-1$ dipole moment parameters. Therefore, the dipole matrix is characterized by $(N^2-N)/2+N-1=(N+2)(N-1)/2$ parameters. Combining the energy and dipole matrix parameters, there are a total of $(N+2)(N-1)/2+N-1$ parameters.

The N -state sum rules are of the form

$$\sum_{n=0}^{\infty} \left(E_n - \frac{1}{2}(E_m + E_p) \right) \langle m|x|n \rangle \langle n|x|p \rangle = \frac{\hbar^2 N}{2m} \delta_{m,p}, \quad (7)$$

so the sum rules comprise a total of N^2 equations [i.e., an equation for each (m, p)]. If the sum rules are truncated to N states, the sum rule indexed by $(m=N, p=N)$ is nonsensical because it contradicts the other sum rules. Furthermore, if the transition moments are real, then $x_{mp} = x_{pm}$, so only $(N^2 - N)/2$ of the equations are independent. As such, there are a total of $(N^2 - N)/2 + N - 1 = (N+2)(N-1)/2$ independent equations.

Since the SOS expression for the nonlinear-susceptibility has $(N+2)(N-1)/2 + N - 1$ parameters and the sum rules provide $(N+2)(N-1)/2$ equations, the SOS expression can be reduced to a form with $N-1$ parameters. For example, the three-level model for the hyperpolarizability, which is expressed in terms of seven parameters, can be reduced to two parameters using five sum rule equations. In practice, however, even fewer sum rule equations are usually available because some of them lead to physically unreasonable consequences. While the (N, N) sum rule is clearly unphysical due to truncation, sum rule equations that are near equation (N, N) may also be unphysical. In the case of the three-level model, it is found that Eqs. (2) and (1) allow for an infinite hyperpolarizability, so that equation is ignored on the grounds that it violates the principle of physical soundness [12,21,26]. This leads to a hyperpolarizability in terms of three variables, which are chosen to be E_{10} , $E = E_{10}/E_{20}$, and $X = x_{10}/x_{10}^{\max}$. The expression is then maximized with respect to the two parameters E and X , leaving the final result a function of E_{10} .

We conclude that the SOS expression for the hyperpolarizability can be expressed in terms of at least $N-1$ parameters so it would appear that as more levels are included in the SOS expression, there are more free parameters that can be varied without violating the sum rules. As $N \rightarrow \infty$, there are an infinite number of adjustable parameters. So, it is indeed puzzling that the three-level ansatz yields a fundamental limit that is consistent with all of our calculations for a wide range of potentials, many of which have many excited states. It may be that we are only considering a small subset of potential energy functions or, perhaps the expression for the hyperpolarizability depends on the parameters in such a way that large matrix elements contribute to the hyperpolarizability with alternating signs so that the big terms cancel. This is a puzzle that needs to be solved if we are to understand what makes β large.

The matrix elements and energies, as summarized by Table II, may hold the key to explaining the puzzle. First, we note that the energy ratio $E \equiv E_{10}/E_{20} \approx 1/2.05$ and that the ratio $X \equiv x_{10}/x_{\max} \approx 0.789$ for the optimized potential for every starting potential. The three-level ansatz, which is used to calculate the fundamental limits reduces to the simple relationships [14]

$$\beta_{\text{int}} = f(E)G(X), \quad (8)$$

where

$$f(E) = (1 - E)^{3/2} \left(E^2 + \frac{3}{2}E + 1 \right) \quad (9)$$

and

$$G(X) = \sqrt[4]{3} X \sqrt{\frac{3}{2}(1 - X^4)}. \quad (10)$$

Using the results from Table II, we get $f(1/2.05) = 0.722$ and $G(0.789) = 0.995$ yielding $\beta_{\text{int}} = 0.72$. The optimized potentials for all starting potentials, yield $\beta_{\text{int}} \approx 0.71$. So, we find that the matrix elements are all optimized according to the three-level ansatz, and, the energy spacing is not optimized, but reminiscent of the spacing in a clipped harmonic oscillator (CHO). So, it seems that when the hyperpolarizability is calculated from a potential energy function, the energy level spacing appears to depend on the dipole matrix elements. When the dipole matrix is optimized, the energy level spacing cannot get larger than what is found for the CHO. That is, when the potential energy is tuned to optimize β_{int} , the energy level spacing cannot be increased while keeping X optimized.

Since the optimized values of β_{int} of all the systems studied are so well characterized by Eq. (8), it would imply that all potentials lead to a three-level system. The top part of Fig. 8 plots the matrix elements for the optimized potential with starting potentials of $V(x) = x + 10 \sin x$ and $V(x) = x^2$. The former leads to an optimized potential with wiggles and well-separated wave functions while the latter leads to a smooth potential with highly overlapping wave functions. Note that in these plots, the diagonal elements x_{nn} have been set to zero for clarity. (These elements are normally much larger than the off-diagonal ones, and overshadow the structure in the off-diagonal elements.)

To study the significance of the contributions of the excited states, we define β_{nm} , the contribution from states n and m to the SOS sum [27]

$$\beta_{nm} = \frac{x_{0n} \bar{x}_{nm} x_{m0}}{E_{n0} E_{m0}}, \quad (11)$$

where $\bar{x}_{nm} \equiv x_{nm} - x_{00} \delta_{n,m}$. The bottom portion of Fig. 8 shows a plot of β_{nm} . The sharp positive peak in each plot is the contribution of the diagonal term of the dominant state n while the smaller negative peaks correspond to the off diagonal term that includes coupling between the dominant state and the subdominant one. The contributions of all other states is negligible.

We find similar behavior for all other potentials: While the dipole moments and transition moments are large for many states, only three states (two excited states and the ground state) contribute to the hyperpolarizability. Thus, all optimized potentials are distinct functions with associated wave functions that are very different for the various potentials leading to very different transition moments and energies, but they all share the common property that they lead to a three-level model for the hyperpolarizability. So, the optimized hyperpolarizability is a three-level model, confirming the three-level ansatz.

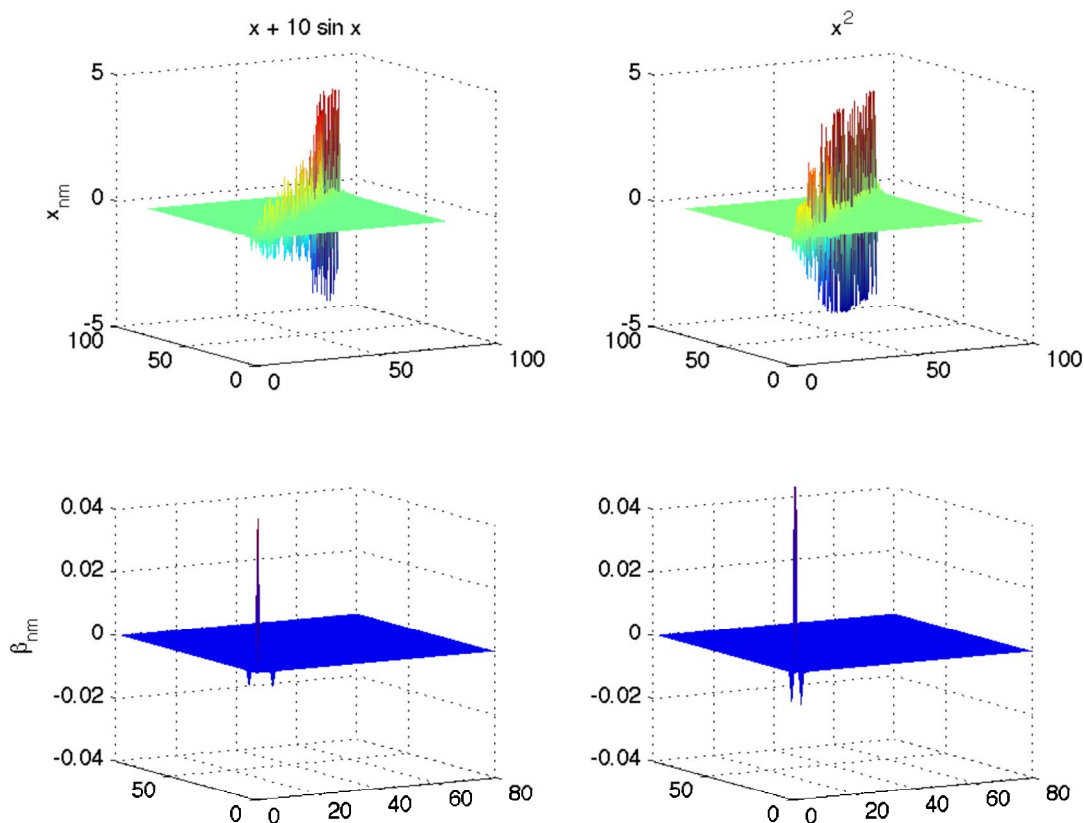


FIG. 8. (Color online) (Top) The x_{nm} matrix elements for the optimized potentials using $V(x)=x+10 \sin x$ and $V(x)=x^2$ as the starting potentials. (Bottom) β_{nm} for each of the plots above.

One might argue that perhaps our numerical methods are in violation of the sum rules. However, Table II shows that both the ground-state sum rule ($\tau_{00}^{(80)}$) and the deviations from all the sum rules combined ($\Delta\tau^{(80)}$) are negligible.

The intriguing conclusion from these sets of observations is that while the set of optimized potential energy functions are all very different from each other, they all share the same energy ratio E and the same normalized transition moment X . Furthermore, the hyperpolarizability is well approximated by the three-level ansatz. So in a sense, from the perspective of the intrinsic hyperpolarizability, all of these potentials are intimately related.

To investigate whether the limiting behavior is due to our use of one-dimensional potentials, we have also optimized the intrinsic hyperpolarizability in two dimensions. In this case, we focus on the largest tensor component β_{xxx} and describe the potential as a superposition of point charges. As described in the literature [19], we solve the two-dimensional Schrödinger eigenvalue problem

$$-\frac{\hbar^2}{2m}\nabla^2\Psi + V\Psi = E\Psi, \tag{12}$$

for the lowest ten to 25 energy eigenstates, depending on the degree of convergence of the resulting intrinsic hyperpolarizability. We use the two-dimensional logarithmic Coulomb potential, which for k nuclei with charges q_1e, \dots, q_ke located at points $s^{(1)}, \dots, s^{(k)}$ is given by

$$V(s) = \frac{e^2}{L} \sum_{j=1}^k q_j \ln\|s - s^{(j)}\|, \tag{13}$$

where L is a characteristic length. With $L=2 \text{ \AA}$, the force due to a charge at distance 2 \AA is the same as it would be for a 3D Coulomb potential.

We discretize the eigenvalue problem given by Eq. (12) using a quadratic finite element method [22,28] and solve the resulting matrix eigenvalue problem for the ten to 25 smallest energy eigenvalues and corresponding eigenvectors by the implicitly restarted Arnoldi method [23] as implemented in ARPACK [29]. Each eigenvector yields a wave function Ψ_n corresponding to energy level E_n . The moments

$$x_{mn} = \int_{-\infty}^{\infty} \int_{-\infty}^{\infty} s_1 \Psi_m(s_1, s_2) \Psi_n(s_1, s_2) ds_1 ds_2$$

are computed, and these and the energy levels E_n are used to compute β .

Figure 9 shows the intrinsic hyperpolarizability of a two-nucleus molecule plotted as a function of the distance between the two nuclei and nuclear charge q_1 . The total nuclear charge is $q_1+q_2=+e$, and is expressed in units of the proton charge e . Three extrema are observed. The positive peak parameters are $\beta_{\text{int}}=0.649$ for $q_1=0.58$ and $d=4.36 \text{ \AA}$. The negative one yields $\beta_{\text{int}}=-0.649$ for $q_1=0.42$ and $d=4.36 \text{ \AA}$. The local negative peak that extends past the graph

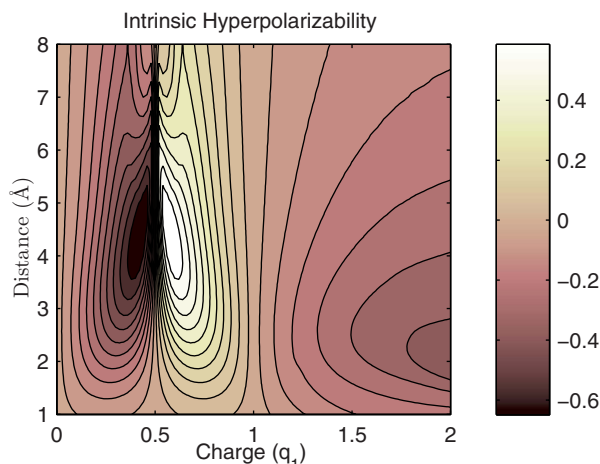


FIG. 9. (Color online) The intrinsic hyperpolarizability of two nuclei as a function of the distance between them and the charge of one nucleus q_1 , where $q_1 + q_2 = +e$.

on the right reaches its maximum magnitude of $\beta_{\text{int}} = -0.405$ at $q_1 = 2.959$ and $d = 2.0$ Å.

Applying numerical optimization to the intrinsic hyperpolarizability using the charges and separation between the nuclei as parameters, we get $\beta_{\text{int}} = 0.654$ at $d = 4.539$ Å, and $q_1 = 0.430$ when the starting parameters are near the positive peak and $\beta_{\text{int}} = -0.651$, $d = 4.443$ Å, and $q_1 = 0.572$ when optimization gives the negative peak. The peak parameters are the same within roundoff errors when optimization or plotting is used, confirming that the optimization procedure yields the correct local extrema.

Figure 10 shows the intrinsic hyperpolarizability of an octupolarlike molecule made of three evenly-spaced nuclei on a circle plotted as a function of the circle's diameter and charge fraction ϵ . $q = \epsilon e$ is the charge of one of the nuclei and the charge on each of the other two nuclei is $e(1 - \epsilon)/2$. The positive peak at $\epsilon = 0.333$ and diameter $D = 6.9$ Å has a hyperpolarizability $\beta_{\text{int}} = 0.326$, while $\beta_{\text{int}} = -0.605$ for a charge fraction $\epsilon = 0.44$ and a diameter $D = 6.8$ Å.

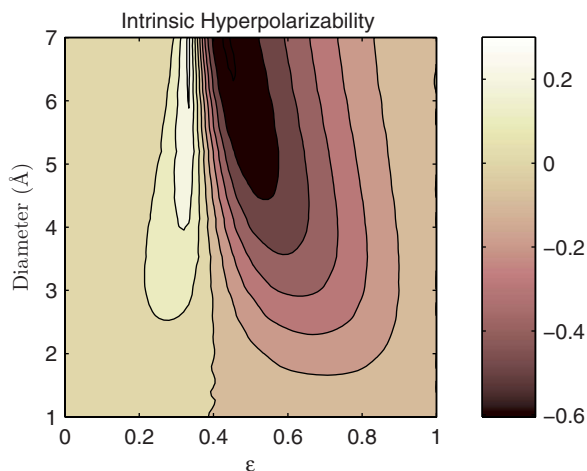


FIG. 10. (Color online) The intrinsic hyperpolarizability of three evenly spaced nuclei on a circle as a function of the circle's diameter and the charge ϵ (in units of e) on one of the nuclei. The charge on each of the other nuclei is $e(1 - \epsilon)/2$.

When the positions and magnitudes of the three charges are allowed to move freely, the best intrinsic hyperpolarizability obtained using numerical optimization is $\beta_{\text{int}} = 0.685$ for charges located at $\vec{r}_1 = (0, 0)$, $\vec{r}_2 = (-4.87 \text{ Å}, 0.33 \text{ Å})$, and $\vec{r}_3 = (-9.57 \text{ Å}, -0.16 \text{ Å})$; with charges $q_1 = 0.43e$, $q_2 = 0.217e$, and $q_3 = 0.351e$. There are only small differences in the optimized values of β_{int} depending on the starting positions and charges; and the best results are for a “molecule” that is nearly linear along the x direction. So, the xxx component of β_{int} is optimized when the molecule is one dimensional. This suggests that one-dimensional systems may have the largest intrinsic hyperpolarizability.

The two-dimensional analysis illustrates that numerical optimization correctly identifies the local maxima (peaks and valleys) and that the magnitude of maximum intrinsic hyperpolarizability (0.65 vs 0.68) is close to the maximum we get for the one-dimensional optimization of the potential energy function (0.71). All computations we have tried, including varying the potential energy function in one dimension or moving around point charges in a plane all yield an intrinsic hyperpolarizability that is less than 0.71.

An open question is the origin of the factor-of-30 gap between the best molecules and the fundamental limit, which had remained firm for decades through the year 2006. Several of the common proposed explanations, such as vibronic dilution, have been eliminated [14]. Perhaps it is not possible to make large-enough variations of the potential energy function without making the molecule unstable. Or, perhaps there are subtle issues with electron correlation, which prevents electrons from responding to light with their full potential. The fact that the idea of modulation of conjugation has led to a 50% increase over the long-standing ceiling—reducing the gap to a factor of 20—makes it a promising approach for further improvements. Continued theoretical scrutiny, coupled with experiment, will be required to confirm the validity of our approach.

IV. CONCLUSIONS

There appear to be many potential energy functions that lead to an intrinsic hyperpolarizability that is near the fundamental limit. These separate into two broad classes: One in which wiggles in the potential energy function forces the eigenfunctions to be spatially separated and a second class of monotonically varying wave functions with small or no wiggles that allow for many strongly overlapping wave functions. The smooth potential functions may be better implemented in stacked structures that are made using molecular beam epitaxy while the wiggly potentials may be more easily reduced to practice in molecules with modulation of conjugation.

When the potential energy function is optimized, the maximal hyperpolarizability is found to be dominated by two excited states. While many of the wave functions may be strongly overlapping, the proportion of the oscillator strength allocated between the two dominant states is such that all other excited states contribute negligibly. Furthermore, the ratio of energies between the two dominant states are the same for all optimized potentials, suggesting that once the

transition moments are optimal, the energy levels cannot be arbitrarily adjusted so that the largest intrinsic hyperpolarizability is 0.71.

Our calculations suggest that one-dimensional molecules have larger values of β_{xxx}^{int} than two-dimensional ones. Perhaps, one-dimensional systems are the best. Interestingly, all these one-dimensional “molecules” have the same maximal intrinsic hyperpolarizability of 0.71 while the 2D systems are all below about 0.68. A second open question pertains to the origin of the long-standing factor of 30 gap between the fundamental limit and the best molecules. The idea of conjugation modulation may be one promising approach for making wiggly potential energy profiles that lead to molecules that fall into the gap. Given that there are so many

choices of potential energy functions that lead to maximal intrinsic hyperpolarizability, it may be possible to engineer many classes of exotic molecules with record intrinsic hyperpolarizability. However, we caution that all of our calculations consider only single-electron systems, and electron correlations may lead to behavior that is different than what we have found here.

ACKNOWLEDGMENTS

M.G.K. thanks the National Science Foundation Grant No. (ECS-0354736) and Wright Paterson Air Force Base for generously supporting this work.

-
- [1] Q. Y. Chen, L. Kuang, Z. Y. Wang, and E. H. Sargent, *Nano Lett.* **4**, 1673 (2004).
- [2] B. H. Cumpston, S. P. Ananthavel, S. Barlow, D. L. Dyer, J. E. Ehrlich, L. L. Erskine, A. A. Heikal, S. M. Kuebler, I.-Y. S. Lee, D. McCord-Maughon, J. Qin, H. Rockel, M. Rumi, X.-L. Wu, S. Marder, and J. W. Perry, *Nature (London)* **398**, 51 (1999).
- [3] S. Kawata, H.-B. Sun, T. Tanaka, and K. Takada, *Nature (London)* **412**, 697 (2001).
- [4] A. Karotki, M. Drobizhev, Y. Dzenis, P. N. Taylor, H. L. Anderson, and A. Rebane, *Phys. Chem. Chem. Phys.* **6**, 7 (2004).
- [5] I. Roy, O. T. Y., H. E. Pudavar, E. J. Bergey, A. R. Oseroff, J. Morgan, T. J. Dougherty, and P. N. Prasad, *J. Am. Chem. Soc.* **125**, 7860 (2003).
- [6] M. G. Kuzyk, *Opt. Lett.* **25**, 1183 (2000).
- [7] M. G. Kuzyk, *IEEE J. Sel. Top. Quantum Electron.* **7**, 774 (2001).
- [8] M. G. Kuzyk, *Phys. Rev. Lett.* **85**, 1218 (2000).
- [9] M. G. Kuzyk, *Opt. Lett.* **28**, 135 (2003).
- [10] M. G. Kuzyk, *Phys. Rev. Lett.* **90**, 039902(E) (2003).
- [11] M. G. Kuzyk, *J. Nonlinear Opt. Phys. Mater.* **13**, 461 (2004).
- [12] M. G. Kuzyk, *J. Chem. Phys.* **125**, 154108 (2006).
- [13] M. G. Kuzyk, *Opt. Photonics News* **14**, 26 (2003).
- [14] K. Tripathi, P. Moreno, M. G. Kuzyk, B. J. Coe, K. Clays, and A. M. Kelley, *J. Chem. Phys.* **121**, 7932 (2004).
- [15] B. J. Orr and J. F. Ward, *Mol. Phys.* **20**, 513 (1971).
- [16] J. Pérez Moreno, Y. Zhao, K. Clays, and M. G. Kuzyk, *Opt. Lett.* **32**, 59 (2007).
- [17] J. Zhou, M. Kuzyk, and D. S. Watkins, *Opt. Lett.* **31**, 2891 (2006).
- [18] M. G. Kuzyk, *Phys. Rev. A* **72**, 053819 (2005).
- [19] M. G. Kuzyk and D. S. Watkins, *J. Chem. Phys.* **124**, 244104 (2006).
- [20] D. Kincaid and E. W. Cheney, *Numerical Analysis: Mathematics of Scientific Computing*, 3rd ed. (Brooks-Cole, Pacific Grove, CA, 2002).
- [21] M. G. Kuzyk, *J. Nonlinear Opt. Phys. Mater.* **15**, 77 (2006).
- [22] O. C. Zienkiewicz, R. L. Taylor, and J. Z. Zhu, *The Finite Element Method: Its Basis and Fundamentals*, 6th ed. (Butterworth-Heinemann, London, 2005).
- [23] D. C. Sorensen, *SIAM J. Matrix Anal. Appl.* **13**, 357 (1992).
- [24] J. C. Lagarias, J. A. Reeds, M. H. Wright, and P. Wright, *SIAM J. Optim.* **9**, 112 (1998).
- [25] B. Champagne and B. Kirtman, *Phys. Rev. Lett.* **95**, 109401 (2005).
- [26] M. G. Kuzyk, *Phys. Rev. Lett.* **95**, 109402 (2005).
- [27] M. C. Kuzyk and M. G. Kuzyk, e-print arXiv:0708.1219.
- [28] K. Atkinson and W. Han, *Theoretical Numerical Analysis, a Functional Analysis Framework* (Springer, New York, 2001).
- [29] R. B. Lehoucq, D. C. Sorensen, and C. Yang, *ARPACK Users' Guide: Solution of Large-Scale Eigenvalue Problems with Implicitly Restarted Arnoldi Methods* (SIAM, Philadelphia, 1998).